

# Exo-Glove Pinch: A Soft, Hand-Wearable Robot Designed Through Constrained Tendon Routing Analysis

Byungchul Kim , *Member, IEEE*, Useok Jeong , and Kyu-Jin Cho , *Member, IEEE*

**Abstract**—Developing tendon-driven soft hand-wearable robots requires reducing the actuator counts to manage system complexity and functionality. Researchers have leveraged the tendons' inherent ability to apply position or force constraints to the joints, enabling the use of fewer actuators. Considering these constraints is important as they significantly affect the robot's motion characteristics such as adaptability and force capability. In this letter, we introduce the Exo-Glove Pinch, which utilizes two active tendons—a flexor and an extensor—to assist individuals with spinal cord injuries (SCI) in performing power grasps (enclosing objects with adaptable motion) and pinch grasps (applying sufficient contact force at the fingertip). By co-contracting the flexor and extensor, the system expands achievable joint torque manifolds, increasing maximum fingertip force by changing the direction of the contact force as verified through analysis and simulation. Preliminary testing with an individual with a spinal cord injury (SCI) suggests that the proposed robot is a promising solution for assisting in grasping variously shaped objects with adaptable power grasps and improving pinch grasp strength, generating fingertip forces 1.36 times greater than the previous actuation strategy.

**Index Terms**—Tendon/wire mechanism, wearable robotics, mechanism design, soft robot applications, rehabilitation robotics.

## I. INTRODUCTION

ADVANCEMENTS in sensing, actuation, and control technologies have significantly expanded the scope of robotic applications. Among these, soft hand-wearable robots have emerged to assist individuals with spinal cord injuries (SCI), stroke, or cerebral palsy, enhancing their quality of life by supporting essential hand functions [1], [2], [3], [4], [5]. For these robots, usability—affected by size, weight, and complexity—is just as crucial as performance, emphasizing the need for comfortable, practical solutions.

To manage system complexity, researchers have focused on reducing the number of actuators while maintaining performance in soft hand-wearable robots. From this perspective, tendon transmission has become popular due to its ability to make motions with fewer actuators [6], [7], [8], [9], [10]. However, unlike fully actuated systems, tendon-driven systems with fewer actuators face limitations in independently controlling joint positions or forces. These design approaches introduce constraints that cause adaptability issues (Fig. 1(a)) [11] and fingertip force capability issues (Fig. 1(b)) [12].

While increasing the number of actuators could alleviate these limitations, the challenge lies in finding the right balance between reducing actuators and ensuring appropriate motion capabilities. However, most prior work has concentrated on minimizing actuator numbers, often neglecting issues such as adaptability and fingertip force capabilities.

In this letter, we introduce the Exo-Glove Pinch, a soft hand-wearable robot designed to assist with two essential grasps: power grasp, which encloses objects through adaptable motions to create multiple contact points, and pinch grasp, which generates a perpendicular force on the contact plane with sufficient force capabilities. The robot achieves these motions through co-contractions of two tendons: a flexor, and an extensor. Further analysis and simulations validate that this tendon configuration enables adaptable movements with sufficient force capabilities. In a case study with an individual with a SCI, it demonstrated the ability to assist in grasping diverse objects with adaptable power grasps and to enhance pinch grasp strength, generating fingertip forces 1.36 times greater than the previous actuation strategy.

## II. PREVIOUS WORKS

**Constrained Tendon Routing:**<sup>1</sup> The underlying principle behind reducing the number of actuators is constraining the

<sup>1</sup>Readers may be more familiar with a term *under-actuated tendon routing* [13], [14] rather than *constrained tendon routing*. However, we use a term

Received 24 March 2025; accepted 26 July 2025. Date of publication 13 August 2025; date of current version 28 August 2025. This article was recommended for publication by Associate Editor M. Bianchi and Editor K.-U. Kyung upon evaluation of the reviewers' comments. This work was supported in part by the National Research Foundation of Korea (NRF) funded by the Korean Government (MSIT) under Project RS-2023-00208052 and Project RS2024-00357718, and in part by Korea Health Technology R&D Project through Korea Health Industry Development Institute (KHIDI), funded by the Ministry of Health & Welfare, Republic of Korea under Grant HI19C1352. (Corresponding author: Kyu-Jin Cho.)

This work involved human subjects or animals in its research. Approval of all ethical and experimental procedures and protocols was granted by Seoul National University Institutional Review Board, under Application No. IRB No. 22014/001-004 and performed in line with the Declaration of Helsinki.

Byungchul Kim is with the Biorobotics Laboratory, School of Mechanical Engineering / Soft Robotics Research Center (SRRC) / IAMD / Institute of Engineering Research, Seoul National University (SNU), Seoul 08826, South Korea, and also with the Distributed Robotics Laboratory, Computer Science and Artificial Intelligence Laboratory, Massachusetts Institute of Technology, Cambridge, MA 02139 USA.

Useok Jeong is with SNU, Seoul 08826, South Korea. He is now with Hyundai Motor Company, Seongnam-si 13529, South Korea.

Kyu-Jin Cho is with the Biorobotics Laboratory, School of Mechanical Engineering / Soft Robotics Research Center (SRRC) / IAMD / Institute of Engineering Research, Seoul National University (SNU), Seoul 08826, South Korea (e-mail: kjcho@snu.ac.kr).

Details can be found at the project website <https://sites.google.com/view/constrained-tendon-routings>

Digital Object Identifier 10.1109/LRA.2025.3598647

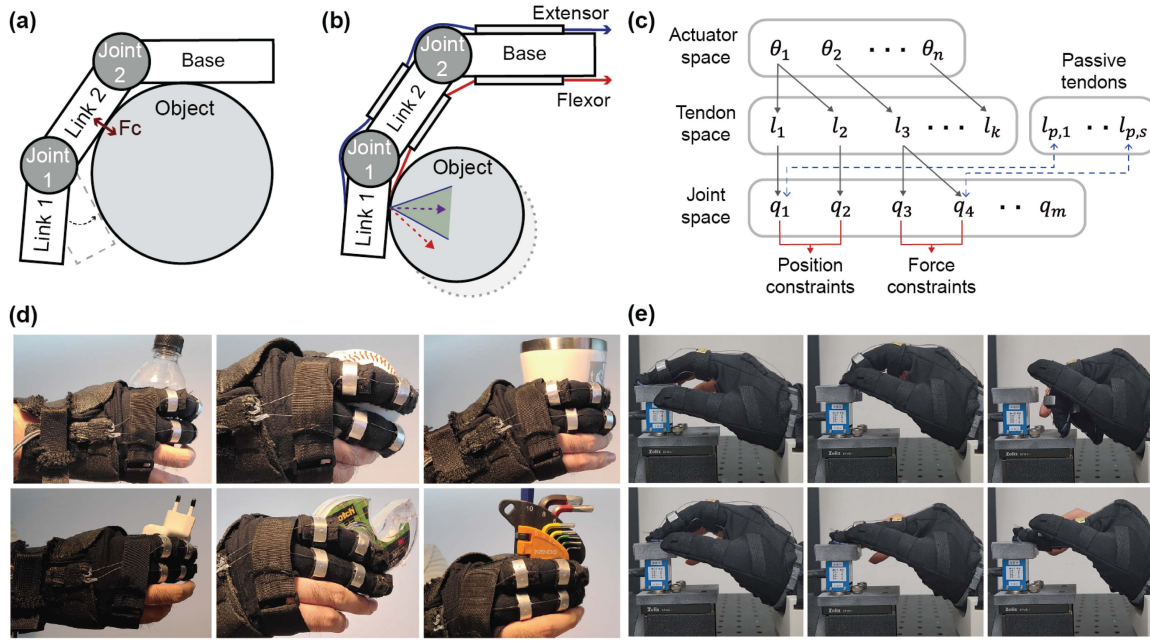


Fig. 1. Addressing adaptability and force capability issues in robots with fewer actuators. (a) Position constraints at the joints lead to adaptability issue—when Link2 is blocked, Link1 cannot move under this constraint type; force constraints should be used to solve this issue as will be explained in section 2. (b) Force constraints raise force capability issues—limited control over fingertip force direction may cause objects to slip from the hand. (c) These issues arise from the constraints applied by the tendon, which is inherent in designs with fewer actuators. (d) The proposed robot only applies force constraints, allowing adaptable power grasp (upper images) and adaptable pinch grasp (lower images). (e) Co-contraction of the flexion and extension tendons prevents slippage and generates sufficient fingertip force. The upper images show slipping when only the flexor is used, while the lower images show the finger not slipping against the force sensor with co-contraction of the tendons.

joints [15]. When the actuator pulls tendons with a motor, each tendon length is predetermined causing position constraints. If the actuator pulls a single tendon that passes multiple joints, the tendon imposes force constraints on the joints as the tendon remains the same in the tendon (Fig. 1(c)). From this perspective, we can categorize tendon routings for fewer actuator use into *position-constrained tendon routings* (PTR) or *force-constrained tendon routing* (FTR) depending on constraints applied to the joints. These routings have shown different motion characteristics as they apply different types of constraints to the joints. This letter aims to develop a soft hand-wearable robot by thoroughly understanding these routings, referred to as *constrained tendon routing*.

**Force-constrained Tendon Routing:** An intuitive example of this routing is a routing that pulls serially connected joints with a single tendon. The tendon remains the same within the tendon, so the force applied to the joints is the same. These routings are known by various names, including under-actuated tendon routing [13], [14], tendon transmission with series transmission matrix [16], differential mechanism [17], [18], and adaptive synergy [19].

Robots using FTR generate unique motion pattern, known as *adaptable* motion, when interacting with the external environment. This pattern is useful in applications related to grasping motion by increasing the number of contact points [20], [21].

*constrained tendon routing* to encompass a broader range of tendon routings. Under our definition, under-actuated tendon routing falls within the category of FTR since it imposes force constraints on the joints. In contrast, constrained tendon routing, which includes both FTR and PTR, captures a wider spectrum of tendon routing approaches with fewer actuators. It would be also inaccurate to categorize PTR as under-actuated tendon routing, because PTR directly reduces the system's degrees of freedom (DOF) rather than utilizing the redundant DOFs.

Therefore FTR has been used in robotic gripper, prosthetic hand, and hand-wearable robots. However, these routings require careful consideration of achievable torque manifolds because joint torque is not fully controllable [15]. The limited manifold may induce the lack of force capability.

**Position-constrained Tendon Routing:** Another routing method pulls multiple tendons with an actuator. This routing, known as *postural synergy* [6], [19] or *branch tendon* [22], is inspired by patterns of human movement [23]. These constraints are implemented by pulling multiple tendons with a set of spools connected in parallel [6], [19] or tying them into a single tendon [22]. This routing has benefits in controlling joint angles as the excursion length of each tendon can be strictly defined from the radii of motor spools.

**Application to single/multi fingered robot:** In practical applications, researchers have preferred FTR over PTR when applying it to the robots with single-finger due to its simplicity and effectiveness—i.e., FTR is easily implemented by pulling a tendon that passes through the joints and also enable the robotic system to generate adaptable motions.

For multi-finger setups, two distinct approaches have been used. The first approach actuates all joints across the fingers using a single tendon, similar to the FTR method. Therefore, the tendon imposes force constraints on all joints within individual fingers and between fingers. We term this routing as *Force-Force-constrained Tendon Routing (F-FTR)* in alignment with other nomenclatures used in this letter as it enforces force constraints both within and across fingers. F-FTR can be implemented by using various design methods including movable pulleys [24], fixed pulleys at the end of linkages (known as *augmented adaptive synergy* [19], [25] or *soft tendon routing* [13]), and specific actuation modules [26], [27].

However, these approaches have suffered from practical issues such as size, friction, and elongation issues due to the complex tendon routings [28]. Recently, a method of combining both fixed pulleys and remote mechanisms, known as Dual-Tendon Routing, has been proposed to overcome the above practical issues [28].

The second approach increases the number of tendons actuated by a motor, akin to methods used in PTR. Each tendon only actuates the joints of a single finger, while the system can actuate multiple fingers by pulling multiple tendons with a motor. This routing is referred to as Position-Force-constrained Tendon Routing (*P-FTR*) in this letter, as it enforces force constraints within joints in each finger while introducing position constraints across fingers. P-FTR has garnered interest because it allows for the actuation of multiple fingers without complicating tendon routing, merely by adding more tendons. However, P-FTR limits the adaptability of motion due to the additional position constraints imposed across the system.

P-FTR can be used to make bidirectional motion [3], [29], [30] or to make motions of multiple fingers [9], [10], [31]. In some cases, researchers have even developed their robot to make the bi-directional motion of multiple fingers using only a single motor with this routing [6].

*Distinction from Prior Work:* Our prior works [3], [13], [28] primarily focused on generating adaptable grasp postures using under-actuated tendon routing, particularly for power grasps. More recent studies [5], [32] introduced diverse thumb postures using additional actuators or position constraints, but continued to emphasize posture generation over stable contact force application.

In contrast, the present work enhances contact force after posture formation through co-contraction of flexor and extensor tendons, validated in both simulation and real-robot experiments. This enables both power and pinch grasps without increasing system complexity, offering improved versatility and grasp stability beyond prior efforts.

*Extension tendon for grasp stabilization:* Biomechanical studies on human hand motion have revealed an interesting observation that humans use extensors to stabilize their grasps [33]. This observation provides us with a hypothesis that we can also develop the robot to stabilize the grasp with an extensor. The Exo-Glove Pinch is developed from this hypothesis as it was proven by our analysis and simulations.

### III. ANALYSIS ON CONSTRAINED TENDON ROUTING

This section presents an analysis to help understanding the actuation characteristics of constrained tendon routing to use them when developing the robot. It starts by defining the tendon Jacobian [14], [16], which represents the relationship between the joint and the actuator position as

$$\dot{\mathbf{l}} = \mathbf{J}_j \dot{\mathbf{q}} + \mathbf{R} \dot{\boldsymbol{\theta}} \quad (1)$$

where,  $\mathbf{l} \in \mathbb{R}^{n \times 1}$ ,  $\mathbf{J}_j \in \mathbb{R}^{n \times N}$ ,  $\mathbf{q} \in \mathbb{R}^{N \times 1}$ ,  $\mathbf{R} \in \mathbb{R}^{n \times m}$ , and  $\boldsymbol{\theta} \in \mathbb{R}^{m \times 1}$  are the tendon length, tendon jacobian, joint angle, radius of the motor spool, and motor displacement, respectively.  $n$ ,  $N$ , and  $m$  are the number of tendons, the number of joints, and the number of motors, respectively. We assume that  $m$  is smaller than  $N$ , as this letter focuses on methods for reducing the number of motors.

#### A. Adaptability

The robot with FTR has fewer tendons than the number of joints. Therefore, the tendon Jacobian in (1) has a null space. Consequently, the infinitesimal change in joint angle ( $d\mathbf{q}$ ) is defined as

$$d\mathbf{q} = \mathbf{J}_j^\dagger \mathbf{R} d\boldsymbol{\theta} + \alpha N(\mathbf{J}_j) \quad (2)$$

where  $N(\mathbf{A})$  and  $\mathbf{A}^\dagger$  represent null space and pseudo-inverse of the matrix  $\mathbf{A}$ , respectively.  $\alpha$  is arbitrary real number that represents *span* of the null-space and it is determined by the contact torque applied by the external environment [14].

Therefore, the postures of robots using FTR are not fully defined by motor positions. While this may poses challenges in certain scenarios, researchers have found clever ways to leverage the existence of null space. They have used this null space to create a unique motion pattern known as *adaptable motion* when interacting with the external environment. For instance, joints can continue to move even if other joints are blocked thanks to the null space of the jacobian (Fig. 1(b)). This adaptability is particularly beneficial in robotic grasping, where it helps increase the number of contact points between the robot and the object, leading to a more stable grasp with force closure.

However, the system using PTR is not adaptable to the external environment because the null space of the tendon Jacobian does not exist. Therefore, all joint angles are strictly determined by motor displacement, and remain unaffected by external forces. In contrast, the robots using FTR face challenges in achieving precise postures since joint positions are governed by force equilibrium. Consequently, they are highly affected by external forces such as friction and gravity. PTR, on the other hand, enables the robot to create accurate posture due to the well-defined kinematic relationship between actuator position and joint angle.

#### B. Force Capability

Adaptability in robots can be thought of as their ability to adjust the motions in response to external environments. However, this characteristic does not always produce the desired outcome. For instance, when grasping flat, cube-shaped objects (e.g., books, tablets, plates, trays, laptops), increasing tendon tension may not stabilize a grasp by either creating adaptive motion or increasing contact force. Instead, the increased tension could cause the object to slip out of the hand (Fig. 1(e)). The capacity to generate sufficient contact force without slipping is known as *force capability* [34].

To increase the contact force without slipping, it's important to consider the direction of the contact force. The force must be directed within the friction cone to prevent sliding on the object. However, in systems with fewer actuators, controlling the force direction becomes challenging due to the limited controllability. For instance, when using a tendon to actuate two joints, the joint torques can be expressed as

$$\begin{aligned} \boldsymbol{\tau}_r &= \mathbf{J}_j^T \mathbf{T} \\ &= [\mathbf{r}_1 \mathbf{T} \quad \mathbf{r}_2 \mathbf{T}]^T. \end{aligned} \quad (3)$$

Consequently, it may not always be possible to generate the exact joint torque required to direct the contact force within the friction cone.

Force capability can also be understood through a achievable torque manifold, representing a set of joint torques the robot can generate in torque space. When only a single flexor is used, as inferred from (3), the manifold is expressed as a straight line



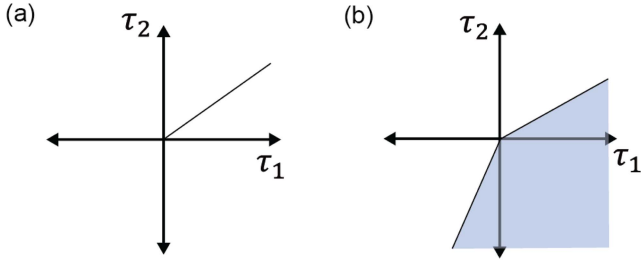


Fig. 2. Achievable torque manifolds in joint torque space. (a) shows the mechanically achievable torque manifold when using a single flexor, while (b) shows the torque manifold (blue region) achievable with both a flexor and an extensor.

in the joint torque space (Fig. 2(a)). If the joint torque, to keep the contact force within the friction cone, does not lie on this realizable torque manifold (straight line in this case), the grasp may become unstable.

The issue of insufficient force capability may be addressed by optimizing the design parameters of the robot [15]. However, this approach is not suitable in tendon-driven soft hand-wearable robot (TSHR) for the following reasons: 1) estimating appropriate contact points—key parameters in optimization—is challenging as the user, not the robot, controls the arm’s movement toward the object; 2) even if the design parameters are optimized under certain assumptions, the results may not be effective in wearable robots since joint stiffness fluctuates with wrist position, which the robot cannot control.

#### IV. METHODS

##### A. Exo-Glove Pinch Development

The analysis in section III provides insights into improving TSHR. As shown in Fig. 2, using both flexor (which assists in flexing the fingers by applying positive joint torque) and extensor (which assists in extending the fingers by applying negative joint torque) significantly expands the achievable torque manifolds. Based on this insight, we developed an improved version of the Exo-Glove [13], incorporating two tendons to enhance the robot’s force capability (Fig. 1(e)).

Section III-A demonstrates that removing position constraints is beneficial for achieving adaptable motions. For this reason, we used F-FTR to route the extensor, whereas our previous design used P-FTR. In our earlier development [13], we preferred P-FTR as the extensor was not used during grasp; it was only used to return the hand to fully extended posture and the position constraint improved posture accuracy at that moment. However, in the current design, where the extensor is used even during grasping, we opted for F-FTR to enhance adaptability. Accordingly, the robot can assist with adaptable power grasps (upper images of Fig. 1(d)) and adaptable pinch grasps (lower images of Fig. 1(d)).

Building on the tendon routing strategies obtained from the analysis, the Exo-Glove Pinch is developed with practical design features as follows. It is designed to actively assist the index/middle fingers (using F-FTR) as this approach has been proven to be beneficial for assisting individuals with SCI [3]. Both flexor and extensor are actuated by Slider-Tendon Linear actuators [26] that are located away from the glove using Bowden cable to simplify the wearing part. For flexor routing (Fig. 3(f)), Dual-Tendon Routing [28], a variant of F-FTR, is implemented as it applies low friction and elongation at the

tendon compared to other F-FTR methods. Conversely, extensor routing (Fig. 3(g)) employs F-FTR with a remotely located actuator [26], chosen for its simplicity in implementation. While this routing may cause issues under high-tension actuation due to elongation, this is not a concern for the extensor as it operates under low tension [28].

A passive thumb fixation unit (red boundaries in Fig. 3) was fabricated using thermoplastic fabric as its benefits have been proved in our previous works [3]. Furthermore, metal routers (green boundaries in Fig. 3) are used in place of soft routers, providing greater actuation stability [35]. This approach addresses the potential deformation of routing caused by the co-contraction of tendons.

##### B. Simulation Conditions for the Validation

1) *Model Definition*: We developed a TSHR model for the simulation with following simplifications: 1) The glove is assumed to be tightly attached to the user’s body; 2) The ring and little fingers are excluded, as they are not actuated in the proposed robot; 3) The thumb is fixed in a specific position, reflecting its fixed state in our robot; 4) The finger sizes are based on measurements from our experimental participant and 5) The mass and joint stiffness of the fingers are defined according to previous biomechanics studies [36], [37]. The simulation was conducted using MuJoCo, a widely used platform that supports tendon-driven actuation [38].

2) *Simulation Condition - Adaptability*: The first simulation examines how position/force constraints affect adaptability when grasping objects of varying sizes and shapes. Here, F-FTR and P-FTR are validated, as they are the major routings used in TSHRs. We simulated two key metrics: 1) the number of contact points and 2) the scalar sum of the contact force at these points. This is because they are closely related to the grasp stability and the force closure [39], [40].

We used only sphere and cylinder shapes, omitting the cube shape structure. This is because the contact at the vertices or edges became unstable when applying position constraints between tendons; the constraints were implemented using MuJoCo’s internal function. In addition to the basic structures, we combined them to create more complex structures, resulting in 6 objects (Fig. 4(a)–(f)) for the simulation.

3) *Simulation Condition - Force Capability*: Previous analyses show that FTRs may experience unstable grasp due to the limited force capability. This usually happens when grasping cube-shaped objects with some ranges of thickness as explained in section III-B. Our solution is using an extensor in grasping because it sufficiently expands the achievable torque manifold. Therefore, we simulated how extensor control can enhance the force capability by using two robots: a robot that only pulls the flexor and a robot that also sets the extensor’s tension to be 85% of the flexor’s tension. This ratio was chosen after testing different ratios through the simulation and selecting the one that maximized the contact force. The maximum contact force was measured when the robots grasped the box (Fig. 4(g)) with different thicknesses (increasing in 5 mm increments from 10 to 70 mm). Since we didn’t simulate P-FTR, simulating with the box shape didn’t cause issues.

4) *Simulation Condition - Grasp Performance*: The proposed robot’s ability to assist with power and pinch grasps allows users to select the appropriate grasp based on an object’s size and shape. If the hand can fully enclose an object, a power grasp provides greater contact points, enhancing grasp stability. Conversely, for flat, cube-shaped objects, a pulp pinch grasp is

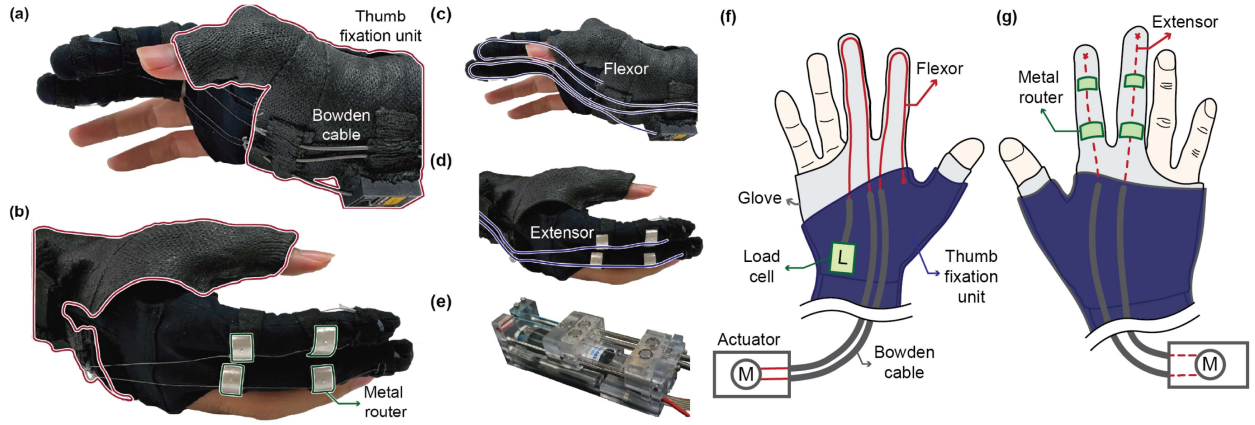


Fig. 3. Exo-Glove Pinch designed to assist with power grasp, enabling object enclosure through adaptable motions, and pinch grasp, providing sufficient contact force via tendon co-contraction. (a) and (b) show the overall view of the robot; (c) and (d) show the flexor and extensor tendon routing, respectively. (e) shows the actuator used for the robot. Tendon is connected to the actuator through the Bowden cable. The red boundaries highlight the thumb fixation unit, which stabilizes the thumb passively; green boundaries indicate the metal routers ensuring stable extensor routing. (f) and (g) provide schematic representations of the robot. In practical use, the thumb is fixed in the opposition position using the fixation unit as shown in (a) and (b); however, in the schematic, it is shown in a repositioned state for better visualization of other components. The letter ‘M’ in the actuator means movable pulley.

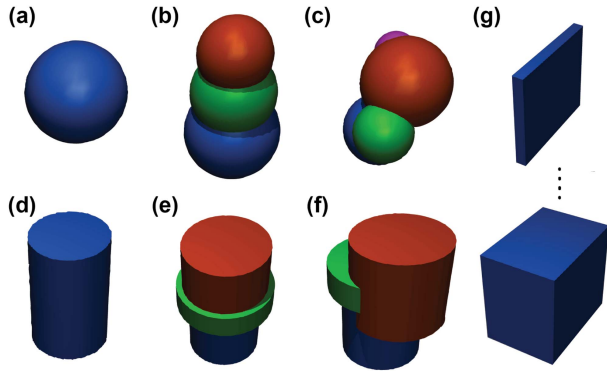


Fig. 4. Objects used for simulation. (a)–(f) are used for adaptability simulation and named as Obj1–Obj6, respectively, in the paper. (g) show cube-shaped objects (a total of 13 objects) used for force capability simulation. The thickness ranges from 10 mm to 70 mm in 5 mm increments.

more effective, as it applies opposing directional forces between the thumb and other fingers.

To further validate the Exo-Glove Pinch’s effectiveness in assisting both grasp types, we evaluated its performance across 19 objects—the same set used in adaptability and force capability tests—using two key performance metrics: resistance to external impact perturbations, which assesses dynamic grasp stability, and the ability to lift heavy objects, which evaluates quasi-static grasp strength.

The first metric quantifies how well the grasp maintains stability under sudden impacts. To evaluate this, an external force of 100 N was applied for 0.5 seconds in the  $\pm x$ ,  $\pm y$ , and  $\pm z$  directions except for the  $-z$  direction because the presence of the ground at  $z = 0$  prevented meaningful assessment. Grasp stability,  $S_{dynamic}$ , is defined as

$$S_{dynamic} = F\Delta T/d \quad (4)$$

where  $F$ ,  $\Delta T$ , and  $d$  represent impact force, impact duration, and displacement, respectively. The object’s displacement was measured by comparing its position before and after impact. The final grasp stability score was obtained by averaging results across five impact directions.

The second metric evaluates the system’s static grasp stability by measuring its capacity to sustain high forces under prolonged

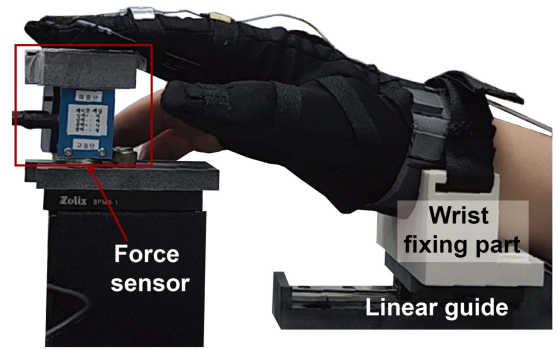


Fig. 5. Experimental setup to measure the force capability. A force sensor measures fingertip force, while a wrist fixing part prevents unwanted voluntary motion of the participant.

loading. To assess this, a virtual force was applied in the  $+z$  direction and gradually increased until the object exhibited significant displacement. The force at which the object’s  $z$ -directional displacement exceeded half its height was recorded as the static grasp stability metric ( $S_{static}$ ); although the gravity direction is  $-z$ , we used  $+z$  directional force as there was a ground plane at  $z = 0$ .

### C. Real-World Experiment Condition

An experiment was conducted with an individual with a SCI (male, C5-6 injured, 39 years old) who was unable to move his hands, to assess whether the robot can assist in grasping with better force capability. All procedures were approved by the Institutional Review Board of SNU (IRB No. 22014/001-004). Using the experimental setup shown in Fig. 5, we measured fingertip force with a single-axis force sensor (333FB Cell, Ktoyo Co., Ltd., Korea) during the robot’s assistance in two different modes. The participant’s wrist was fixed to the fixation unit that can move horizontally, preventing any unintended forces from wrist motion. The passive thumb fixation unit was removed in this setup to avoid interference.

The experiments are conducted 10 times with extensor control and 10 times without it. During the trials with extensor control, the tension of the extensor was consistently maintained at 5 N by

TABLE I  
SIMULATION RESULT MEASURING THE ADAPTABILITY OF THE MOTION

		Obj1	Obj2	Obj3	Obj4	Obj5	Obj6
Contact points (#)	P-FTR	4	5	4	3	4	4
	F-FTR	6	6	8	5	5	5
Contact Force (N)	P-FTR	143.6	218.3	163.0	100.4	139.2	117.5
	F-FTR	338.6	629.5	517.2	537.5	396.1	358.3

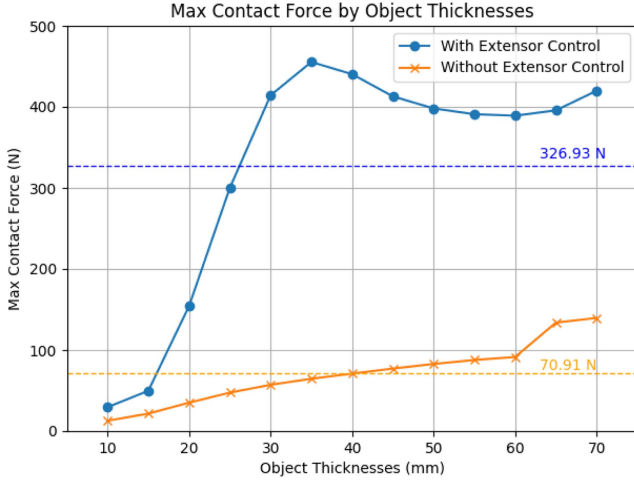


Fig. 6. Simulation results for the force capability. Maximum contact force is measured to validate the force capability. Each dotted line shows the average results from different object sizes.

controlling the motor. This tension level was chosen heuristically through several experiments, as it showed better results than our initial modeling, which did not fully account for complex friction forces.

## V. RESULTS

### A. Adaptability and Force Capability Validation in Simulation

Table I illustrates the differences in adaptability between the robot with P-FTR and that with F-FTR. The P-FTR robot achieves an average of 4 contact points with a contact force of 147.0 N, whereas the F-FTR robot achieves 5.8 contact points with a contact force of 462.9 N. We can find that F-FTR achieves more contact points and a higher contact force.

Fig. 6 shows the maximum contact force measured when grasping cube-shaped objects of varying thickness under two different controls. The results indicate that extensor co-contraction increases the contact force by 361.05% compared to the case without it. This phenomenon can be explained by differences in grasping postures: with co-contraction, the robot achieves pulp pinch postures (Fig. 7(a)) [41], [42], whereas, without it, the robot creates power grasp postures (Fig. 7(b)). From the torque manifold perspective, when only the flexor is actuated, the robot can generate only positive torque at all joints, similar to Fig. 2(a). In contrast, co-contraction expands the manifold, allowing the robot to apply positive torque to MCP joints while maintaining negative (or zero) torques at other joints.

For cube-shaped objects, achieving a pulp pinch posture (Fig. 7(c)) aligns the fingertip force of the index/middle fingers with that of the thumb, preventing slip and ensuring a stable grasp. However, when only the flexor is used, simultaneous finger joint rotation (Fig. 7(d)) causes the fingers to slide along the object's surface, limiting sufficient contact force.

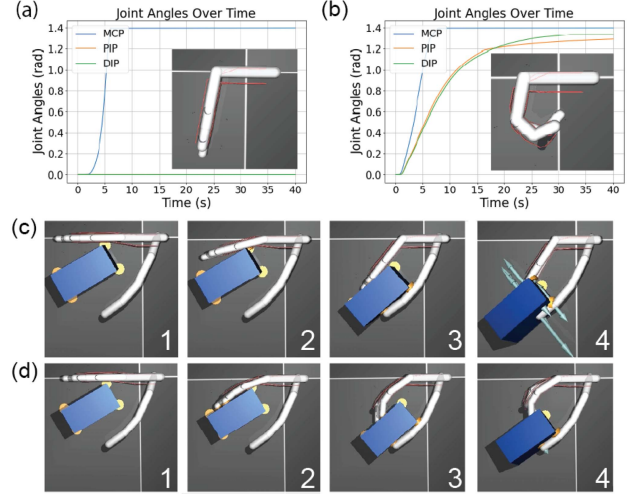


Fig. 7. Grasping with/without extensor co-contraction. (a) and (b) show how the joint moves with and without co-contraction, respectively. (c) and (d) show how the hand grasps the object (that has 50 mm thickness) with and without co-contraction, respectively. Blue arrows at the figures represent the contact force.

### B. Grasp Performance in Simulation

Fig. 8 demonstrates the effectiveness of Exo-Glove Pinch in assisting both power and pinch grasps. When grasping objects 1–6 (used in adaptability test) the power grasp showed greater stability, with dynamic stability improving by 344.55% and static stability by 366.45%. Conversely, for cube-shaped objects, the pinch grasp outperformed the power grasp, achieving a 1496.15% increase in dynamic stability, and a 323.76% improvement in static stability.

### C. Real-World Experiment Results

Fig. 9 illustrates the impact of extensor control on fingertip force. We observed that, without extensor control (w.o. EC), the fingers tended to slip off the force sensors. However, when both tendons were controlled (w. EC), the fingers maintained their position and did not slip. Without extensor control, the maximum fingertip force was only 6.22 N; with the extensor control, the maximum fingertip force increased by 136.01% to 14.68 N. This is evident in Fig. 9(b)—without extensor control, the tendon displacement continuously increases as the fingertip slips, eventually causing the fingertip force to drop to zero as the finger completely loses contact with the sensor. In contrast, with extensor control, the tendon displacement and fingertip force converge to certain values.

We believe that the qualitative feedback from disabled people on their experience with the robots is also important in wearable robot research. According to the person with a SCI participated in the experiment, co-contraction (described as pulling the fingers toward the back of the hand by the participant) increased the pressing force applied to the object and made the contact force feel stronger compared to when the fingers were not pulled back. Please check our <https://sites.google.com/view/constrained-tendon-routings/3-exo-glove-pinch?authuser=0#h.yj6nkpwlxuo4> website (section 3.3) for the interview video.



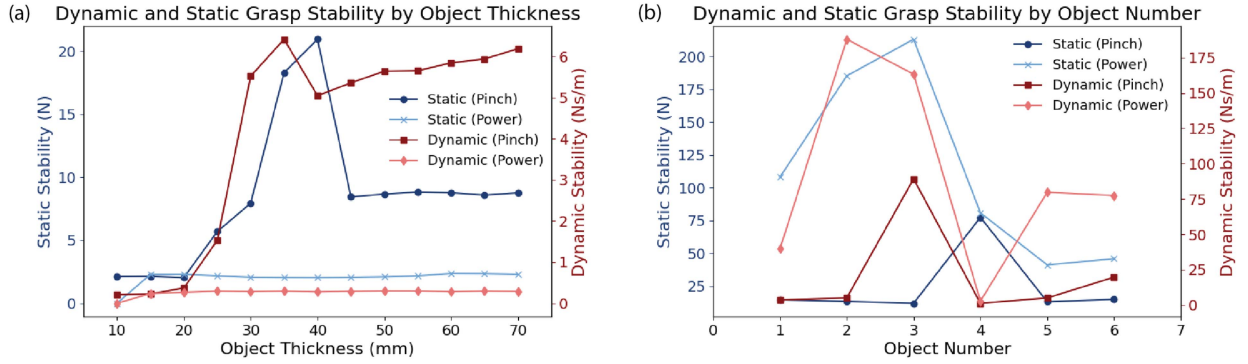


Fig. 8. Dynamic and static grasp stability when assisting with two different grasp modes. (a) results when grasping the objects used in the force-capability test and (b) results when grasping the objects used in the adaptability test. In this simulation, pinch and power grasps are made with and without extensor co-contraction, respectively. The indicators for dynamic and static stability are defined in section IV-B.4.

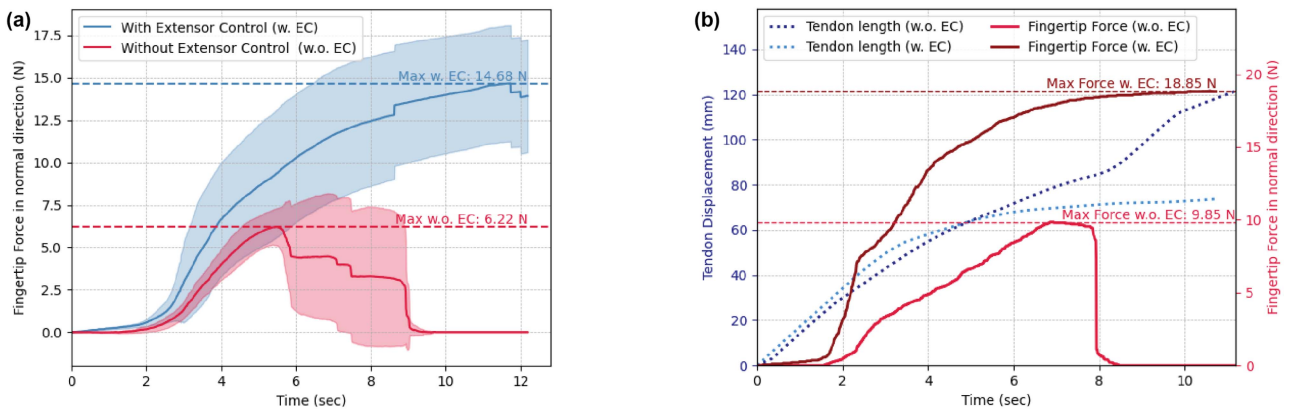


Fig. 9. Effects of extensor control on pinch force assistance. (a) Fingertip force over time with and without extensor control. The experiments were conducted 10 times for each condition. Shaded regions show the standard deviation. (b) Tendon displacement and fingertip force over time for a single experiment, illustrating the differences between the experiments with extensor control (w. EC) and experiments without extensor control (w.o. EC).

## VI. DISCUSSION AND CONCLUSION

This letter proposes the Exo-Glove Pinch developed for individuals with SCI, developed through the understanding of the constrained tendon routings. Building on our previous robots [3], [28] designed solely for assisting power grasps, the proposed robot introduces two key improvements informed by our simulation results (Section V-A). First, we replaced P-FTR with F-FTR for extensor routing to enhance motion adaptability during grasping. The robot with F-FTR setup yielded more contact points than the P-FTR setup, thereby increasing the potential for more stable grasps through improved force closure. Second, the robot assists both power and pinch grasps by leveraging the co-contraction of flexor and extensor. This strategy improves versatility in grasping various object shapes and tasks by exploiting their respective strengths (Fig. 8).

Since the torque generated by the extensor opposes that of the flexor, co-contraction effects may seem counterintuitive. However, extensor tension can help align the contact force within the friction cone, allowing the finger to exert force more normally to the surface without slipping. This can also be understood through finger kinematics. In our robot, the flexor's moment arm at the metacarpophalangeal (MCP) joint is designed to be larger than that of the extensor, while both tendons have similar

moment arms at the other joints. This design strategy allows the co-contraction to flex only the MCP joint while keeping other joints straight, therefore the hand can apply force more normally to the surface (Fig. 7). As a result, the fingers maintain better contact, reducing slippage and enabling the application of greater force.

The hand taxonomy in biomechanic study classifies the grasp posture into the power grasp and the precision grasp [43]. Since grasps in two categories have different purposes and characteristics, it may be beneficial to assist at least two grasp postures (one in the power grasp and one in the precision grasp). From this perspective, we believe Exo-Glove Pinch can improve the users' quality of life by expanding the tasks they can do with their hands as it provides assistance for one grasp in each category.

This study lacks a proper control method for the extensor, primarily due to the difficulty of accurately modeling human-robot interaction given the variability in human body properties. In addition, the experimental validation was limited to a single case study involving an individual with a SCI, which constrains the generalizability of the findings. Future work will focus on developing human-in-the-loop optimization strategies for extensor control and expanding the participant pool to evaluate performance across a broader range of users, and addressing grasp variability to better reflect real-world use cases.

We believe that this work will be a good guideline when building a tendon-driven hand-wearable robot with fewer actuators. With an in-depth understanding of constraints applied to the joints by the tendons, researchers will be able to develop their robots to have proper motion characteristics.

#### ACKNOWLEDGMENT

This work was done at Seoul National University (SNU), Seoul, Korea.

#### REFERENCES

- [1] S. F. M. Toh, K. N. Fong, P. C. Gonzalez, and Y. M. Tang, "Application of home-based wearable technologies in physical rehabilitation for stroke: A scoping review," *IEEE Trans. Neural Syst. Rehabil. Eng.*, vol. 31, pp. 1614–1623, 2023.
- [2] V. Sanchez, C. J. Walsh, and R. J. Wood, "Textile technology for soft robotic and autonomous garments," *Adv. Funct. Mater.*, vol. 31, no. 6, 2021, Art. no. 2008278.
- [3] B. B. Kang, H. Choi, H. Lee, and K. J. Cho, "Exo-Glove Poly II: A polymer-based soft wearable robot for the hand with a tendon-driven actuation system," *Soft Robot.*, vol. 6, no. 2, pp. 214–227, 2019.
- [4] B. Kim, J. Ryu, and K.-J. Cho, "Joint angle estimation of a tendon-driven soft wearable robot through a tension and stroke measurement," *Sensors*, vol. 20, no. 10, 2020, Art. no. 2852.
- [5] K. B. Kim, H. Choi, B. Kim, B. B. Kang, S. Cheon, and K.-J. Cho, "Exo-Glove Poly III: Grasp assistance by modulating thumb and finger motion sequence with a single actuator," *Soft Robot.*, 2025.
- [6] M. Xiloyannis, L. Cappello, K. D. Binh, C. W. Antuvan, and L. Masia, "Preliminary design and control of a soft exosuit for assisting elbow movements and hand grasping in activities of daily living," *J. Rehabil. Assistive Technol. Eng.*, vol. 4, 2017, Art. no. 205566831668031.
- [7] K. Gilday, C. Sirithunge, F. Iida, and J. Hughes, "Embodied manipulation with past and future morphologies through an open parametric hand design," *Sci. Robot.*, vol. 10, no. 102, 2025, Art. no. eads6437.
- [8] W. R. Wockenfuß, V. Brandt, L. Weisheit, and W.-G. Drossel, "Design, modeling and validation of a tendon-driven soft continuum robot for planar motion based on variable stiffness structures," *IEEE Robot. Automat. Lett.*, vol. 7, no. 2, pp. 3985–3991, Apr. 2022.
- [9] S. Park, C. Meeker, L. M. Weber, L. Bishop, J. Stein, and M. Ciocarlie, "Multimodal sensing and interaction for a robotic hand orthosis," *IEEE Robot. Automat. Lett.*, vol. 4, no. 2, pp. 315–322, Apr. 2019.
- [10] S. W. Lee, K. A. Landers, and H. S. Park, "Development of a biomimetic hand exotendon device (BiomHED) for restoration of functional hand movement post-stroke," *IEEE Trans. Neural Syst. Rehabil. Eng.*, vol. 22, no. 4, pp. 886–898, Jul. 2014.
- [11] M. G. Catalano, G. Grioli, E. Farnioli, A. Serio, C. Piazza, and A. Bicchi, "Adaptive synergies for the design and control of the Pisa/IIT SoftHand," *Int. J. Robot. Res.*, vol. 33, no. 5, pp. 768–782, 2014.
- [12] L. Birglen and C. M. Gosselin, "On the force capability of underactuated fingers," in *Proc. 2003 IEEE Int. Conf. Robot. Automat.*, 2003, vol. 1, pp. 1139–1145.
- [13] H. In, B. B. Kang, M. Sin, and K.-J. Cho, "Exo-Glove: A wearable robot for the hand with a soft tendon routing system," *IEEE Robot. Automat. Mag.*, vol. 22, no. 1, pp. 97–105, Mar. 2015.
- [14] M. Kim, J. Park, J. Kim, and M. Kim, "Stiffness decomposition and design optimization of under-actuated tendon-driven robotic systems," in *Proc. 2018 IEEE Int. Conf. Robot. Automat.*, 2018, pp. 2266–2272.
- [15] T. Chen, L. Wang, M. Haas-Heger, and M. Ciocarlie, "Underactuation design for tendon-driven hands via optimization of mechanically realizable manifolds in posture and torque spaces," *IEEE Trans. Robot.*, vol. 36, no. 3, pp. 708–723, Jun. 2020.
- [16] R. Ozawa, H. Kobayashi, and K. Hashirai, "Analysis, classification, and design of tendon-driven mechanisms," *IEEE Trans. Robot.*, vol. 30, no. 2, pp. 396–410, Apr. 2014.
- [17] J. T. Belter and A. M. Dollar, "Novel differential mechanism enabling two DoF from a single actuator: Application to a prosthetic hand," in *Proc. IEEE 13th Int. Conf. Rehabil. Robot.*, 2013, pp. 1–6.
- [18] L. Gerez and M. Liarokapis, "An underactuated, tendon-driven, wearable Exo-Glove with a four-output differential mechanism," in *Proc. 41st Annu. Int. Conf. IEEE Eng. Med. Biol. Soc.*, 2019, pp. 6224–6228.
- [19] C. D. Santina, C. Piazza, G. Grioli, M. G. Catalano, and A. Bicchi, "Toward dexterous manipulation with augmented adaptive synergies: The Pisa/IIT SoftHand 2," *IEEE Trans. Robot.*, vol. 34, no. 5, pp. 1141–1156, Oct. 2018.
- [20] L. Birglen, T. Laliberté, and C. M. Gosselin, *Underactuated Robotic Hands*, vol. 40. Berlin, Germany: Springer, 2007.
- [21] G. Xie, L. Chin, B. Kim, R. Holladay, and D. Rus, "Strong compliant grasps using a cable-driven soft gripper," in *Proc. 2024 IEEE/RSJ Int. Conf. Intell. Robots Syst.*, 2024, pp. 8696–8703.
- [22] D. Sawada and R. Ozawa, "Joint control of tendon-driven mechanisms with branching tendons," in *Proc. IEEE Int. Conf. Robot. Autom.*, 2012, pp. 1501–1507.
- [23] M. Santello, M. Flanders, and J. F. Soechting, "Postural hand synergies for tool use," *J. Neurosci.*, vol. 18, no. 23, pp. 10105–10115, 1998.
- [24] A. M. Dollar and R. D. Howe, "The highly adaptive SDM hand: Design and performance evaluation," *Int. J. Robot. Res.*, vol. 29, no. 5, pp. 585–597, 2010.
- [25] M. G. Catalano, G. Grioli, E. Farnioli, A. Serio, C. Piazza, and A. Bicchi, "Adaptive synergies for the design and control of the Pisa/IIT SoftHand," *Int. J. Robot. Res.*, vol. 33, no. 5, pp. 768–782, 2014.
- [26] B. Kim, U. Jeong, B. B. Kang, and K. J. Cho, "Slider-tendon linear actuator with under-actuation and fast-connection for soft wearable robots," *IEEE/ASME Trans. Mechatron.*, vol. 26, no. 6, pp. 2932–2943, Dec. 2021.
- [27] L. Gerez, J. Chen, and M. Liarokapis, "On the development of adaptive, tendon-driven, wearable Exo-Gloves for grasping capabilities enhancement," *IEEE Robot. Automat. Lett.*, vol. 4, no. 2, pp. 422–429, Apr. 2019.
- [28] B. Kim, U. Jeong, and K.-J. Cho, "Dual-tendon routing: Tendon routing for under-actuated tendon-driven soft hand-wearable robot," *IEEE Robot. Automat. Lett.*, vol. 10, no. 4, pp. 3612–3619, Apr. 2025.
- [29] D. Popov, I. Gaponov, and J. H. Ryu, "Portable exoskeleton glove with soft structure for hand assistance in activities of daily living," *IEEE/ASME Trans. Mechatron.*, vol. 22, no. 2, pp. 865–875, Apr. 2017.
- [30] F. Klug et al., "An anthropomorphic soft exosuit for hand rehabilitation," in *Proc. 16th IEEE Int. Conf. Rehabil. Robot.*, 2019, pp. 1121–1126.
- [31] C. G. Rose and M. K. O'Malley, "Hybrid rigid-soft hand exoskeleton to assist functional dexterity," *IEEE Robot. Automat. Lett.*, vol. 4, no. 1, pp. 73–80, Jan. 2019.
- [32] B. Kim, H. Choi, K. Kim, S. Jeong, and K.-J. Cho, "Exo-Glove shell: A hybrid rigid-soft wearable robot for thumb opposition with an under-actuated tendon-driven system," *Soft Robot.*, vol. 12, no. 1, pp. 22–33, 2024.
- [33] F. J. Valero-Cuevas, J. D. Towles, and V. R. Hentz, "Quantification of fingertip force reduction in the forefinger following simulated paralysis of extensor and intrinsic muscles," *J. Biomech.*, vol. 33, no. 12, pp. 1601–1609, 2000.
- [34] L. Birglen and C. M. Gosselin, "Kinetostatic analysis of underactuated fingers," *IEEE Trans. Robot. Automat.*, vol. 20, no. 2, pp. 211–221, Apr. 2004.
- [35] B. Kim, H. Choi, K. Kim, S. Jeong, and K.-J. Cho, "Exo-Glove shell: A hybrid rigid-soft wearable robot for thumb opposition with an under-actuated tendon-driven system," *Soft Robot.*, vol. 12, no. 1, pp. 22–33, 2025.
- [36] A. Esteki and J. Mansour, "An experimentally based nonlinear viscoelastic model of joint passive moment," *J. Biomech.*, vol. 29, no. 4, pp. 443–450, 1996.
- [37] J. Ma'touq, "An index finger musculoskeletal dynamic model," in *Computer Methods, Imaging and Visualization in Biomechanics and Biomedical Engineering*, G. A. Ateshian, K. M. Myers, and J. M. R. S. Tavares, Eds. Cham, Switzerland: Springer, 2020, pp. 411–436.
- [38] E. Todorov, T. Erez, and Y. Tassa, "MuJoCo: A physics engine for model-based control," in *Proc. IEEE/RSJ Int. Conf. Intell. Robots Syst.*, 2012, pp. 5026–5033.
- [39] D. Prattichizzo and J. C. Trinkle, *Springer Handbook of Robotics*, vol. 46. Berlin, Germany: Springer, 2009.
- [40] V.-D. Nguyen, "Constructing force-closure grasps," *Int. J. Robot. Res.*, vol. 7, no. 3, pp. 3–16, 1988.
- [41] P. K. Ng, M. C. Bee, A. Saptari, and N. A. Mohamad, "A review of different pinch techniques," *Theor. Issues Ergonom. Sci.*, vol. 15, no. 5, pp. 517–533, 2014.
- [42] A. Hara, Y. Yamauchi, and K. Kusunose, "Analysis of thumb and index finger joints during pinching motion and writing a cross, as measured by electrogoniometers," in *Proc. Clin. Biomech. Related Res.*, Springer, 1994, pp. 282–293.
- [43] T. Feix, J. Romero, H.-B. Schmiedmayer, A. M. Dollar, and D. Kragic, "The grasp taxonomy of human grasp types," *IEEE Trans. Hum.-Mach. Syst.*, vol. 46, no. 1, pp. 66–77, Feb. 2016.